Supplement of Atmos. Meas. Tech., 12, 2033–2042, 2019
https://doi.org/10.5194/amt-12-2033-2019-supplement

Atmospheric Measurement Techniques
Open Access
EGU

Supplement of

Effect of dry or wet substrate deposition on the organic volume fraction of core–shell aerosol particles

Hansol D. Lee et al.

Correspondence to: Alexei V. Tivanski (alexei-tivanski@uiowa.edu)

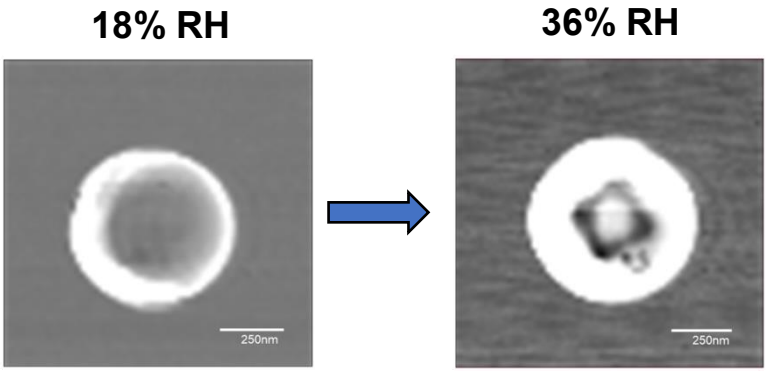

Figure S1. AFM phase images of 1:8 (M) glucose:NaCl particle at varying RH (left - 18% RH, right - 36% RH). Image from 36% RH shows greater contrast between the core and shell, which aided in OVF quantification.

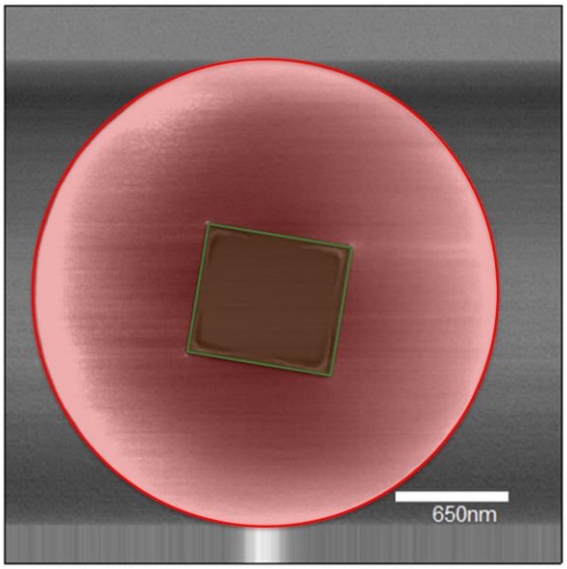

Figure S2. AFM phase image of a sucrose:NaCl particle. Colored regions are masks created in Igor Pro Particle Analysis software, which is transferred onto the 3D height image for volume analysis. The red region indicates the mask used to calculate the total particle volume. The green region indicates the mask used to calculate the core volume. Equation 1 in the main text is used to calculate organic volume fraction.

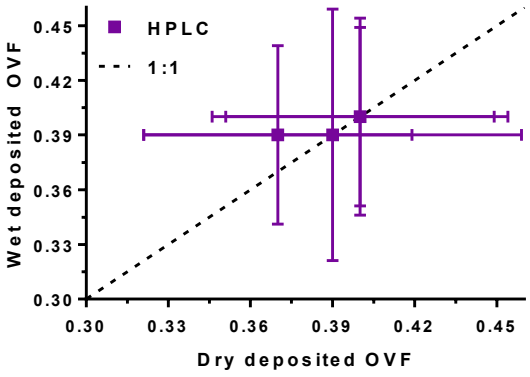

Figure S3. HPLC dry versus wet OVF data for 1:8 (M) glucose:NaCl (purple squares). The dashed black line represents a 1:1 correspondence between the x- and y-axis. The close overlap between the data and expected 1:1 correspondence indicates no significant differences between dry and wet deposition in OVF_{bulk}.

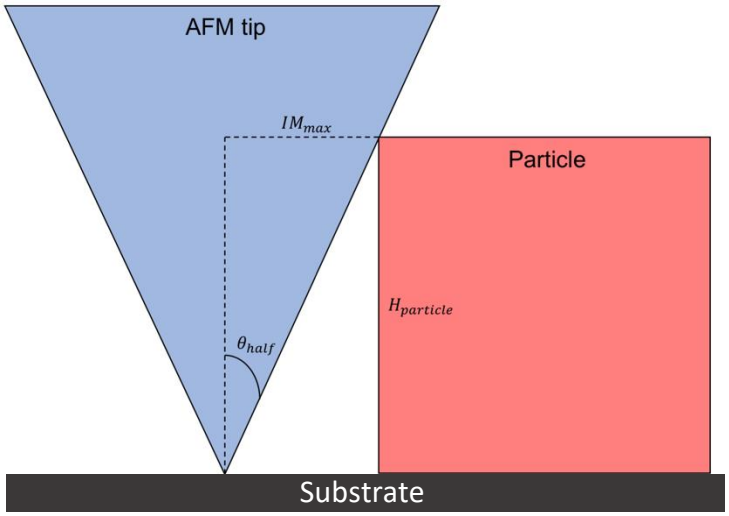

Figure S4. Schematic of AFM tip and core particle, with known θ_{half} and $H_{particle}$, used to calculate IM_{max}. The core is assumed to be rectangular in shape.

Environmental factors that affect AFM phase imaging

In this study, AFM imaging was performed at a relatively low RH range of 25 – 35% to minimize water uptake contribution in organic volume fraction (OVF) measurements, but also still maximize the observed phase separation between the inorganic core and organic shell to facilitate identification of boundaries between two components within a particle. An example of an ideal phase contrast level is shown in Figure S1, where the same particle at 36% RH clearly shows distinct topographical features of the inorganic core, whereas the particle core at 18% RH is not as evident. Here, we define the term "phase bleeding" to describe the lack of distinct inorganic core features that separate it from the organic shell, which is evident on the particle at 18% RH. This phase bleeding likely stems from the relatively high glucose viscosity at this RH, where the smaller difference in viscosity between the core and shell leads to less distinct phase separation. From 18% RH to 36%, a doubling of RH results in two orders of magnitude decrease in the organic component viscosity, with no change in the inorganic component viscosity, which qualitatively aids in better phase separation.[1] NaCl viscosity will be unaffected until reaching a sharp deliquescent point at ~75% RH, at which point a phase transition from solid to liquid results in a many order of magnitude decrease in viscosity. Likewise, the effect of changing temperature would most likely produce similar effects, where the greater difference in viscosity between the core and shell through modulating the temperature could aid in observed phase separation.

Ensemble average OVF comparison between AFM and bulk

To validate our quantitative single particle OVF measurements, a comparison is made to bulk OVF measurements from HPLC, a well-established analytical tool that can measure the concentrations of various compounds in a chemical mixture. In this case, the concentrations of glucose, sodium

and chloride were determined in aqueous extracts of filter samples and were field blank subtracted. Masses of these species were converted to volumes, and used to calculate OVF_{bulk} following Equation S1,

$$OVF_{bulk} = \frac{\frac{m_{org}}{\rho_{org}}}{\frac{m_{org}}{\rho_{org}} + \frac{m_{inorg}}{\rho_{inorg}}} \quad \text{Eq. S1}$$

where OVF_{bulk} is organic volume fraction of bulk, m_{org} & m_{inorg} are masses, and ρ_{org} & ρ_{inorg} are pure solute densities of organic and inorganic components, respectively. Specifically, $\rho_{org} = 1.54\ g/mL$ and $\rho_{inorg} = 2.16\ g/mL$ were used for glucose and NaCl, respectively (Lee et al., 2017). Masses m_{org} and m_{inorg} were obtained by converting the concentrations measured by the HPLC using the sample extract volume to determine the moles of analyte and the molar masses of glucose, sodium and chloride to determine the mass.

HPLC measurement propagated analytical uncertainty

Vertical error bars for HPLC measurements, or bulk, in Figures 2, 4 are propagated analytical uncertainty for each measurement. The absolute error was calculated:

$$e = \sqrt{{\sigma_{FB}}^2 + ([x] * |\%\ spike\ deviation|)^2} \quad \text{Eq. S2}$$

where e is absolute uncertainty, σ_{FB} is standard deviation of field blank, $[x]$ is sample concentration, and $|\%\ spike\ deviation|$ is absolute deviation of spike recovery. When combining errors in propagation, the following was used:

$$e_3 = \sqrt{e_1^2 + e_2^2} \quad \text{Eq. S3}$$

where e_3 is the absolute uncertainty of summed values, and e_1 & e_2 are absolute uncertainties of starting values. Specifically, Equation S3 was used to propagate the error when the mass of sodium and chloride were summed and when the volume of sodium chloride and glucose were summed. To determine the absolute uncertainty in the OVF measurement when division is used, the absolute uncertainty in the volume for glucose and the total volume (glucose+NaCl) was converted to % relative uncertainty:

$$\%e_{OVF} = \sqrt{(\%e_{glucose})^2 + (\%e_{glucose+\,NaCl})^2} \qquad \text{Eq. S4}$$

where $\%e_{OVF}$ is the percent relative uncertainty of OVF, and $\%e_{glucose}$ & $\%e_{glucose+\,NaCl}$ are percent relative uncertainty for glucose and glucose+NaCl volumes, respectively.

Expected OVF calculations

Comparisons to single particle and bulk OVF in the main text are made to the expected OVF, which was calculated by measuring the molar mixing ratio of the bulk solution before and after bubbling, and calculating the volume with known densities of individual components:

$$OVF_{exp} = \frac{V_{org}}{V_{org} + V_{inorg}} = \frac{\chi_{org} * MW_{org} * \rho_{org}^{-1}}{(\chi_{org} * MW_{org} * \rho_{org}^{-1}) + (\chi_{inorg} * MW_{inorg} * \rho_{inorg}^{-1})} \qquad \text{Eq. S5}$$

where OVF_{exp} is expected organic volume fraction, V_{org} & V_{inorg} are volumes, MW_{org} & MW_{inorg} are molecular weights, and χ_{org} & χ_{inorg} are mole fractions of organic and inorganic components, respectively. Specifically, $\rho_{org} = 1.54\ g/mL$ and $\rho_{inorg} = 2.16\ g/mL$ were used for glucose and NaCl, respectively (Lee et al., 2017).

Statistics

Gaussian distributions of OVF data were compared by quantifying the Cohen's d and student's t (Equations S6, S7). The p value, with calculated student's t and degree of freedom, was calculated using the GraphPad Prism software.

$$d = \frac{\overline{x_n} - \mu}{\sqrt{\frac{SD_n^2 + SD_\mu^2}{2}}} \quad \text{Eq. S6}$$

$$t_{calc} = \frac{\overline{x_{n_1}} - \overline{x_{n_2}}}{\sqrt{\frac{SD_1^2}{n_1} + \frac{SD_2^2}{n_2}}} \quad \text{Eq. S7}$$

$$SS_n = \sum (x - \overline{x_n})^2 \quad \text{Eq. S8}$$

where $\overline{x_n}$ is sample mean, μ is population mean, SD is the corresponding standard deviation, n is number of samples, and SS is sum of squares.

To reject the null hypothesis that dry deposited versus wet deposited OVF data are statistically insignificant, an independent samples t-test (dark orange vs. blue) was performed for the 1:8 (M) glucose:NaCl data. This comparison will be used to calculate the probability of obtaining the observed differences from dry versus wet OVF values out of random chance. Also, to quantify how the sample means from dry versus wet deposited OVF data compared to the expected value, Cohen's d was calculated, which represents how far away the sample mean is with respect to the expected value, but normalized to the distributions shown. Equations for t-test and Cohen's d are in the supporting information (Eq. S6 & S7). First, comparing the dry- versus wet-deposited OVF distributions, two tailed t-test confirmed extremely strong statistical significance, $t(354) = 32.838$, $p < 0.0001$. Thus, statistical analysis shows that there is less than 0.01%

probability of random chance that can explain the differences in the sample means. Therefore, t-test confirmed that dry and wet deposited particles produced statistically different results, which allows us to reject the null hypothesis outlined in the beginning. Also, Cohen's d calculations for the dry (dark orange) and wet (blue) OVF data versus the expected value was 4.142 and -0.419, respectively. Therefore, the wet deposited particles were statistically much closer to the expected value then the dry deposited particles.

For 1:2 (M) glucose: NaCl data, comparing the smaller, dry deposited OVF data distribution (light orange) versus wet deposited particles (blue) in Figure 4, two tailed *t*-test confirmed extremely strong statistical significance, $t(228) = -5.596$, $p < 0.0001$. Second, comparing the larger, dry deposited OVF data distribution (dark orange) versus wet deposited particles (blue), *t*-test also confirmed extremely strong statistical significance, $t(243) = 17.751$, $p < 0.0001$. In addition, Cohen's *d* calculations for the smaller, dry deposited OVF data distribution (light orange) versus expected from bulk, was -0.789. The larger, dry deposited OVF data distribution (dark orange) versus expected from bulk, was 2.145. In contrast, the wet deposited particles (blue) versus expected was -0.138.

For Figure 5B, two tailed *t*-test confirmed extremely strong statistical significance between before and after hyd-deh cycle particles, $t(66) = 6.612$, $p < 0.0001$. Also, Cohen's *d* calculations were 2.855 and 0.244 for the particles before and after the hyd-deh cycle, respectively. Moreover, with 99.9% confidence, the mean from after the cycle falls within the confidence interval of the expected value, CI = [0.349, 0.383].

Decoupling AFM tip convolution from NaCl spreading

To validate that the observed width of the NaCl particle data is attributed directly to the NaCl particle spreading and not from AFM particle broadening as a result of convolution of the shape

of AFM tip and shape of the core, an equation was derived to calculate for the maximum width broadening (Fig. S4),

$$IM_{max} = H_{particle} * \tan(\theta_{half}) \qquad \text{Eq. S9}$$

where IM_{max} is maximum imaging width broadening, $H_{particle}$ is height of the core, and θ_{half} is half cone angle of the AFM tip. IM_{max} is inherent to scanning probe microscopy techniques such as AFM, that depend on the probe sharpness and shape. For the AFM tips used in this study, θ_{half} is 20˚, and IM_{max} would be up to 36% of the particle height, or roughly maximum of 180 nm for a particle height of 500 nm. Therefore, the observed 300 nm directional spreading shown in Figure 3B cannot be solely attributed to the width broadening due to the shape of AFM probe, and thus at least 120 nm is directly attributable to NaCl spreading as a result of impaction to the solid substrate.

The data set supporting this manuscript is hosted by the UCSD Library Digital Collections (https://doi.org/10.6075/J04M92SF)

References

Lee, H. D., Estillore, A. D., Morris, H. S., Ray, K. K., Alejandro, A., Grassian, V. H., and Tivanski, A. V.: Direct Surface Tension Measurements of Individual Sub-Micrometer Particles Using Atomic Force Microscopy, J Phys Chem A, 121, 8296-8305, 10.1021/acs.jpca.7b04041, 2017.